Biochimica et Biophysica Acta 818 (1985) 365–372
Elsevier

BBA 72725

The use of cobalt ions as a collisional quencher to probe surface charge and stability of fluorescently labeled bilayer vesicles

Stephen J. Morris [a,*], Diane Bradley [a] and Robert Blumenthal [b]

[a] *Neurotoxicology Section, Laboratory of Experimental Neuropathology, NINCDS, Bldg. 9, Rm. 1E127, and* [b] *Section on Membrane Function, Laboratory of Theoretical Biology, NCI, NIH, Bethesda, MD 20205 (U.S.A.)*

(Received May 13th, 1985)

Key words: Unilamellar vesicle; Co^{2+}; Fluorescence labeling; Membrane surface potential; Fluorescence quenching; Bilayer defect

Co^{2+} quenched the fluorescence of the lipid probes NBD-phosphatidylethanolamine (NBD-PE) and lissamine-rhodamine phosphatidylethanolamine (N-Rh-PE) incorporated into lipid vesicles, according to a collisional quenching mechanism in agreement with the Stern-Vollmer law. The quenching coefficient (Q) for NBD-PE, incorporated into uncharged phosphatidylcholine (PC) vesicles was 13.8 M^{-1}. This value was equal to the quenching coefficient of water-soluble NBD-taurine in aqueous solution, indicating that Co^{2+} was readily accessible to the outer surface of PC vesicles. In phosphatidylserine-phosphatidylethanolamine (PS-PE) (1:1) vesicles, quenching was also proportional to Co^{2+} concentration but Q was 114 mM^{-1}, some 8000-fold smaller. Using the Gouy-Chapman-Stern model we demonstrated that the surface density of Co^{2+} bound to lipid was linear with Co^{2+} concentration in the medium up to 7%. Co^{2+}-associated phospholipid would in turn quench NBD-PE or N-Rh-PE by collisional quenching with lateral diffusion. We investigated the ability of Co^{2+} to permeate PS-PE (1:1) vesicles. Co^{2+} quenched fluorophores on the outer surface of large unilamellar vesicles, formed by reverse-phase evaporation. In small unilamellar vesicles Co^{2+} quenched probes on both outer and inner surfaces, indicating rapid permeation of the ions into the vesicles. Using stopped-flow rapid mixing, we measured the rate of influx of Co^{2+}, and correcting for surface potential using the Gouy-Chapman-Stern model, we calculated a permeability coefficient of 10^{-12} cm/s for Co^{2+} concentrations below 300 μM. Above this concentration, there was a very steep rise in the permeability coefficient, indicating that binding of Co^{2+} induces defects in the bilayer of these vesicles. This may be related to the ability of the vesicles to undergo membrane fusion. A method for calculating the membrane surface potential from Co^{2+} quenching data is presented.

Introduction

Unilamellar vesicles of uniformly relative small size (25–30 nm) can be formed by sonication of phospholipid dispersions in buffer. These particles represent the highest radius of curvature which can be achieved by a bilayer. Simple geometric

* To whom correspondence should be addressed.

Abbreviations: REV, large unilamellar vesicles prepared by reverse-phase evaporation; SUV, small unilamellar vesicles; NBD, *N*-(7-nitrobenz-2-oxa-1,3-diazol-4-yl)amino; N-Rh, lissamine-rhodamine; PC, phosphatidylcholine; PE, phosphatidylethanolamine; PS, phosphatidylserine; Q, Stern-Vollmer quenching coefficient; Hepes, 4-(2-hydroxyethyl)-1-piperazineethanesulfonic acid.

0005-2736/85/$03.30 © 1985 Elsevier Science Publishers B.V. (Biomedical Division)

considerations predict that 65–70% of the phospholipids of such a particle will be located in the outer leaflet [1]. Larger diameter bilayer vesicles of uniform size with lower radius of curvature can be formed by the reverse-phase evaporation technique of Szoka and Papahadjopoulos [2]. Both types of vesicle have been used as models for various aspects of bilayer structure [3]. They have been extensively used in the study of membrane fusion events due to the relative ease of formation, handling, ability to incorporate a variety of probes, and ease of assessing that fusion has taken place [4].

Both small and large unilamellar vesicles can entrap material present in solution at the time of formation. Molecules like carboxyfluorescein incorporated into the interior of vesicles in this manner remain encapsulated for more than a week [5]. We have previously reported that the process of fusion of small unilamellar vesicles formed from equimolar amounts of PS and PE is leaky to small, encapsulated molecules like carboxyfluorescein [6]. We report here that the divalent ion Co^{2+} will easily penetrate the interior of SUV but not REV. The significance of this finding is discussed in relation to the structure of the bilayer and membrane fusion.

In addition to the use of Co^{2+} as a probe for the stability of lipid bilayer vesicles, it is also used as a way to measure the surface charge. This technique can be applied to both artificial and biological membranes.

Materials and Methods

Phospholipids. Phospholipids were purchased from Avanti Polar Lipids, Birmingham, AL, delivered in solid CO_2 and stored at $-20°C$ until used (within 2 months of delivery). Cobalt chloride, purchased from Sigma, St. Louis, MO (lot No. 12F-0343) was made up as a 1.00 M stock in deionized, distilled water and further diluted for use. All other chemicals were of reagent grade. All solutions were prepared with deionized, distilled water containing 10–50 μM Ca^{2+} (as tested by a calcium electrode). Because of the high affinity of Co^{2+} for calcium chelators, no attempt was made to reduce the calcium concentrations below this level.

Preparation of vesicles. Small unilamellar vesicles (SUV) were prepared as described previously [6] using 10 mM Hepes/10 mM KCl/2 mM NaOH (pH 7.2). Large unilamellar vesicles were prepared by modifications of the method of Szoka and Papahadjopoulos [2,6] in the same buffer. Figure legends contain the conditions for each experiment.

Steady-state fluorescence measurements. Fluorescence was measured using a Perkin-Elmer MPF 44B fluorimeter. Materials were added to the curvette in small volumes by hand. No attempt was made to resolve the time-dependent fluorescence changes by hand mixing.

Stopped-flow measurements. These were made using a computer-controlled machine briefly described in Ref. 6. Fluorescence and absorbance changes were recorded simultaneously, using excitation and emission wavelengths of 475/530 and 560/590 nm for NBD and N-Rh, respectively. Data reduction and curve fitting were preformed on the NIH DEC-10 facility using MLAB [7] routines.

Calculations. Fluorescence quenching data were fitted to exponential processes of the type:

$$\Delta F = A_1(1-\exp(-k_1 t)) \tag{1}$$

or:

$$\Delta F = A_1(1-\exp(-k_1 t)) + A_2(1-\exp(-k_2 t)) \tag{2}$$

where A_1 and A_2 are the amplitudes and k_1 and k_2 the initial rates for the change in fluorescence, ΔF.

The changes in apparent absorbance, ΔA, due to Co^{2+}-promoted aggregation of the vesicles was fitted to a single second-order process of the type:

$$\Delta A = A_1 k_1 t/(1+k_1 t) \tag{3}$$

Previous experiments with calcium-promoted aggregation of vesicles required more elaborate models [6,8]. However, in this case aggregation was deliberately kept to a minimum and aggregation probably did not proceed beyond a small amount of dimerization (see below).

Surface-bound cobalt. The concentrations of monovalent and divalent cations at the surface of the membrane $C_i(0)$ are related to their bulk aque-

ous concentrations (C_i) by the Boltzman equation:

$$C_i(0) = C_i \exp(-zF\psi_0/RT) \quad (4)$$

where ψ_0 is the surface potential. Binding of ions to the head groups of phospholipids (P) yielding the ion-phospholipid headgroup complex (C_iP) is given by:

$$C_iP = K_iC_i(0)P \quad (5)$$

where K_i is the binding constant for the ith ion to a given lipid. Those binding constants have been measured for a variety of monovalent and divalent cations to various phospholipids [9]. In order to calculate C_iP we need to know the surface potential ψ_0. This is accomplished by calculating the surface charge. Eqns. 4 and 5 for each ion and each lipid are combined with expressions for conservation of total ionic and lipid species. The resulting Langmuir isotherm combined with the Grahame expression for surface charge gives rise to what is known as the Stern-Gouy-Chapman equation (see Refs. 9 and 10 for a full derivation). This is solved numerically to yield ψ_0 for a given lipid composition as a function of ion concentration in bulk aqueous solution. Knowing ψ_0, we can calculate the amount of a given ion bound to the phospholipid as shown in Fig. 3.

Conversion of the initial rate of cobalt penetration, k_1, into permeability changes were made by applying the Goldman-Hodgkin-Katz equation:

$$P = \frac{k_1 V \exp(\psi_0/K)}{A} \cdot \frac{(1-\exp(\Delta\psi/K))}{(\Delta\psi/K)} \quad (6)$$

where V/A is the volume over the surface area of the vesicles, ψ_0 the surface potential on the outer surface, and $\Delta\psi$ the membrane potential which is essentially the difference between the inner and outer surface potentials [12,13]. The constant $K = zF/RT \simeq 12.85$ mV for Co^{2+}.

Other calculations are described in the text and figure legends.

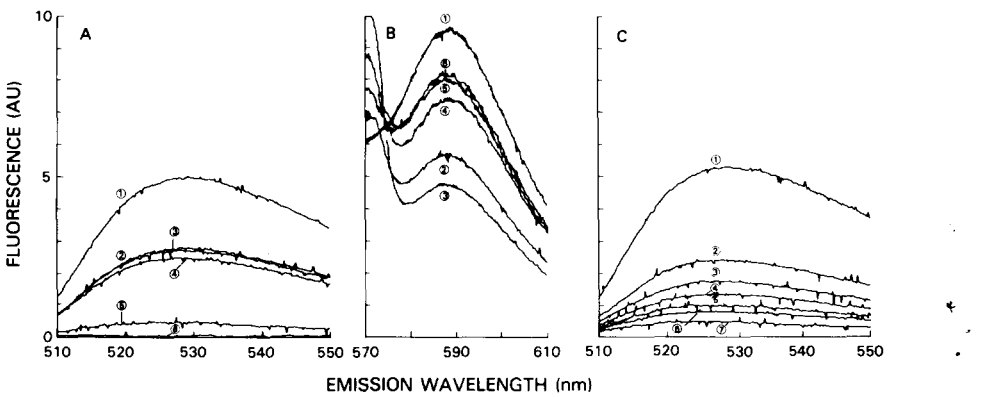

Fig. 1. (A) Co^{2+}-promoted quenching of NBD-PE incorporated into PS-PE REV. Excitation 450 nm, slits 10 nm; temperature 23°C. Titrations were carried out as described in Materials and Methods. (1) NBD-PE containing REV (90 μg lipid/ml). (2) The same sample to which has been added $CoCl_2$ to a final concentration of 0.224 mM. (3) Further increase of $CoCl_2$ to 0.448 mM. (4) Further increase to 1.334 mM. (5) The same sample after freezing and thawing once. (6) The same sample after freezing and thawing four times. (B) Reversal of Co^{2+}-quenching of N-Rh-PE containing REV by use of EDTA. Excitation 570 nm. Slits 10/5 nm. Temperature 23°C. (1) N-Rh-PE-containing REV (48 μg/ml), followed by successive additions of $CoCl_2$ to final concentrations of 0.225 mM (2), 1.334 mM $CoCl_2$, (3) 7.69 mM EDTA (4) 15.38 mM EDTA (5) and 23.07 mM EDTA (6). Direct addition of 7.69 mM EDTA produced a reduction of N-Rh fluorescence equal to the differences between traces 1 and 6 (approx. 10% reduction). Further additions of EDTA had no effect (data not shown). The apparent fluorescence at 570 nm is to a large degree due to scattering of the sample. Note that 0.22 mM Co^{2+} produces only a slight change at this wavelength, indicative of a small amount of aggregations, while 1.33 mM produces extensive aggregation. The reversal of the bulk of the aggregation by EDTA can also be seen. Dimerization of particles of this size should produce an approximate doubling of the turbidity [14,15]. (C) Quenching of NBD-PE in PS-PE SUV by Co^{2+}. Traces from top to bottom represent addition of 0, 0.22, 0.446, 0.656, 0.875, 1.077 and 2.074 mM $CoCl_2$. Experimental conditions as for (A).

Results and Discussion

Penetration of Co^{2+} ions into PS-PE (1 : 1) small and large unilamellar vesicles

Addition of Co^{2+} to NBD- or N-Rh-containing vesicles results in quenching of fluorescence. Fig. 1A shows the titration of NBD-PE containing large unilamellar vesicles (REV) with Co^{2+}. About 60% of the fluorescence is quickly titrated; further additions of Co^{2+} result in little change in fluorescence. This would be the expected result for these 100–200 nm diameter bilayer vesicles if the fluorescent probe were distributed in both leaflets of the bilayer at the same surface density and only the probes in the outer leaflet were quenched. This interpretation is further supported by experiments in which the Co^{2+}-titrated material is frozen and thawed several times (Fig. 1A). This treatment would be expected to break open the vesicles, allowing the Co^{2+} to quench the internal lipids. As can be seen, almost all the fluorescence is quenched by four rounds of freezing and thawing. The quenching of Co^{2+} in unfrozen N-Rh-labeled REV can be reversed approx. 90% by the addition of EDTA, presumably by chelating available Co^{2+} (Fig. 1B). It should be noted that EDTA itself quenches about 10% of the available fluorescence (data not shown).

Fig. 1C shows the titration of NBD-labeled small unilamellar vesicles (SUV) with Co^{2+}. As can be seen, one can eventually quench all of the available fluorescence. Similar results (not shown) can be achieved if N-Rh-PE is used as the fluorophore.

Fig. 2A shows the cobalt-concentration dependence of quenching of NBD-taurine in solutions or NBD-PE cosonicated into PC vesicles plotted according to the Stern-Vollmer collisional quenching model, yielding a quenching coefficient, Q, of 13.8 M^{-1}. This value is about 4-fold smaller than that recently reported by Homan and Eisenberg [11] for NBD-PE incorporated into egg PC large unilamellar vesicles formed by detergent dialysis. We see substantially the same results when titrating in the presence of 145 mM NaCl/10 mM Hepes (pH 7.4) (data not shown), and have no explanation for the difference.

Fig. 2B shows Stern-Vollmer quenching for NBD-PE or N-Rh-PE-containing PS-PE 1 : 1 SUV,

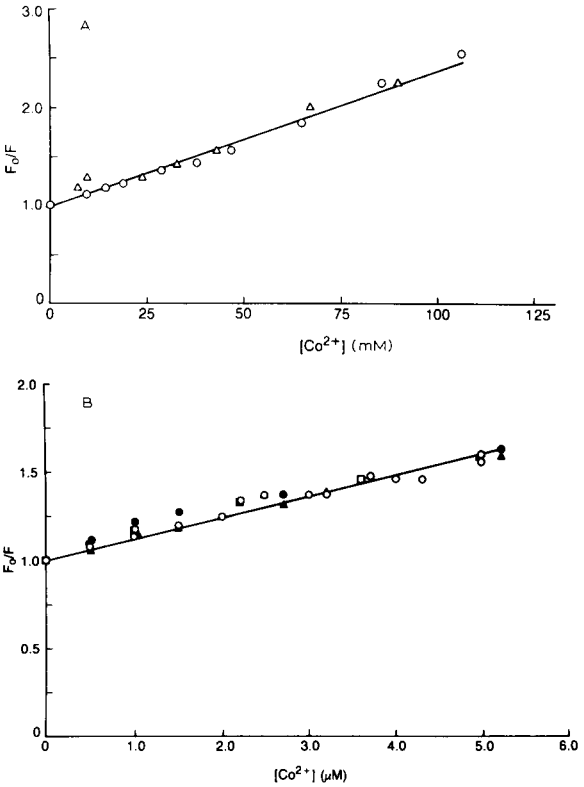

Fig. 2. Determination of Stern-Vollmer quenching coefficients for Co^{2+}. (B) Titration of NBD-PE or N-Rh-PE cosonicated into PS-PE (1 : 1) SUV. Five titrations are plotted for NBD-PE: to labelled phospholipid ratios of 1 : 200 (○), 1 : 100 (□) and 1 : 50 (△), and N-Rh-PE : PL ratios of 1 : 100 (●) and 1 : 50 (▲). The Stern-Vollmer coefficient, Q, is calculated from the relationships $F_0/F = cQ + 1$, where F_0 and F represent unquenched fluorescence and fluorescence at Co^{2+} concentration c. (A) Similar titrations for NBD-taurine (○) and NBD-PE-PC 1 : 100 SUV (△). Data for PC vesicles was corrected assuming that only the outer monolayer of the SUV (representing 65% of the total lipid) was exposed to the quencher.

from which a Stern-Vollmer coefficient for Co^{2+} of 114 mM^{-1} can be calculated. The lower Q for PS-PE is presumably due to the negative surface charge which gives rise to ion accumulation at the vesicle surface as predicted by the Stern-Gouy-Chapman double layer theory. Using the data of McLaughlin et al. [9] for cobalt binding to PS and PC, we have calculated the theoretical surface density of Co-lipid complexes. Fig. 3 shows that the percentage of Co-associated lipid is linearly proportional to Co^{2+} in the medium up to about 7

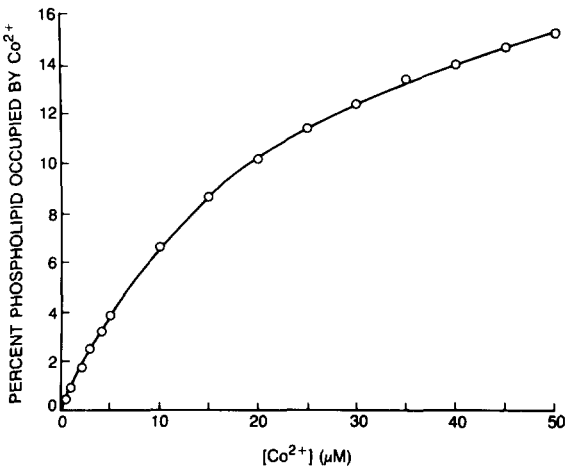

Fig. 3. Theoretical plot of percent of surface of a PS-PE 1:1 vesicle occupied by Co-PS complexes. Points on the curve were calculated from the data in Fig. 2 according to the Stern-Gouy-Chapman theory [9], using a binding constant for Co-PS of 28 M^{-1}, in 10 mM K^+/2 mM Na^+/50 μM Ca^{2+}. The binding constant of Co^{2+} to PE is not known. Since the constant for Co-PS is about twice that for Ca-PS, we have taken $K_{Co\text{-}PE} = 6\ M^{-1}$, about twice $K_{Ca\text{-}PE}$. The binding constants for Ca^{2+}, Na^+ and K^+ were also taken from Ref. 9.

μM. If we assume that collisional quenching is proportional to the Co-lipid surface density, we can interpret this as Co-lipid complexes interacting with the NB-PE by lateral diffusion followed by collisional quenching. At the relative low surface density of the complexes, this quenching is linearly proportional to the surface concentration of the Co^{2+}-bound lipid.

Kinetics of cobalt permeability into SUV

The kinetics of Co^{2+} quenching were investigated by stopped-flow rapid mixing. Changes in the turbidity and fluorescence of the samples were followed simultaneously [6]. The fluorescence quenching results for the SUV are presented in Fig. 4A and Table I. The fluorescence changes can be described by three processes: by triggering before mixing, we could demonstrate that quenching of the REV occurred with half-times which were within the 3 ms dead-time of the stopped-flow mixing apparatus (data not shown). A similar change was seen for the SUV. The very end of this process can be seen in the beginning of the records for the lowest concentrations of cobalt. We interpret this to represent the quenching of the outer leaflet of the bilayer membrane. No other change was observed for REV.

The SUV showed a second time-resolvable process which could be fit to a single exponential of

TABLE I

RATES AND AMPLITUDES FOR BOTH COBALT-PROMOTED QUENCHING OF FLUORESCENCE AND AGGREGATION OF PS-PE (1:1) SMALL UNILAMELLAR VESICLES

Data were fitted to Eqn. 1 for fluorescence through to 300 μM Co^{2+}, to Eqn. 2 for higher Co^{2+} concentrations. Fitted values had errors of less than 5% in all cases. The absorbance data were fitted to Eqn. 3. Errors as noted were large due to the very low amplitudes. Due to the noise in the experiment at 400 μM Co^{2+}, no fit was attempted. Other experimental points marked (–) denote failure of the fitting routines to converge after ten iterations. AU, arbitrary units. Note: All concentrations of Co^{2+} resulted in a process too fast to measure, with an amplitude of about 15 AU for 25 μM Co^{2+}.

$[Co^{2+}]$ (μM)	Fluorescence quenching				Aggregation	
	A_1 (AU)	k_1 (10^{-2} s^{-1})	A_2 (AU)	k_2 (10^{-3} s^{-1})	A_1 (10^{-5} A_{560})	k_1 (10^{-2} s^{-1})
25	–	–	–	–	–	–
50	–	–	–	–	–	–
75	−7.5	2.08	–	–	–	–
100	−19.6	1.23	–	–	–	–
200	−15.9	2.16	–	–	–	–
300	−20.1	7.77	–	–	4.95	2.93
400	−18.0	45.0	−0.91	3.18	–	–
500	−21.0	77.6	−1.56	76.4	7.76	10.2
600	−34.1	129	−1.14	125	5.00	66.9
700	−33.0	261	−1.22	205	8.08	32.2
800	−32.9	381	−1.28	236	8.91	28.9

the type described in Eqn. 1 for cobalt concentrations from 75 to 300 μM. Above 300 μM the data were well described by two exponentials (Eqn. 2).

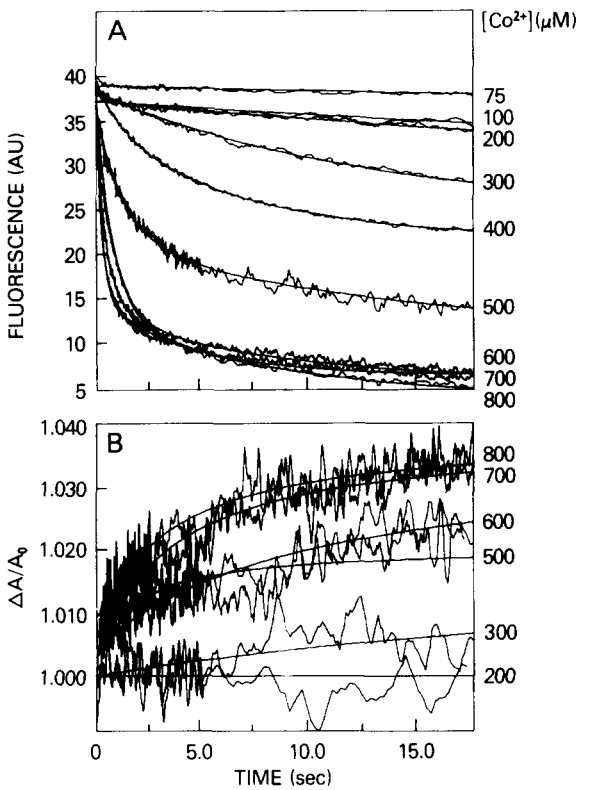

Fig. 4. Progress of cobalt quenching and aggregation of PS-PE 1:1 small unilamellar vesicles by stopped flow mixing. Experiments were performed by rapidly mixing N-Rh-PE labelled PS-PE vesicles (final lipid concentration 96 μg/ml) against $CoCl_2$ solutions at the final concentrations noted. (A) The normalized raw data and fitted curves. Data taken at 25 and 50 μM Co^{2+} had zero slopes and have been omitted for clarity. However, comparisons of the fluorescence signals before and after mixing showed that about 30% of the fluorescence was quenched within the mixing time. The remaining data have been normalized to start at an arbitrary value of 100. Data taken at 75, 100, 200 and 300 μM were fitted to Eqn. 1. The data at 400, 500, 600, 700 and 800 μM were fitted to Eqn. 2. The fitted rates and amplitudes are listed in Table I. (B) Simultaneous measurement of aggregation by changes in apparent absorbance at 560 nm [6,8,15] showed no change for Co^{2+} concentrations below 200 μM. The data for low concentrations are omitted, being essentially the same as those for 200 μM. Higher concentrations produced small increments in turbidity indicative of a small amount of aggregation. These data were fitted to Eqn. 3. The data for 400 μM Co^{2+} contained an artifact which precluded fitting and are not included. The rates and amplitudes are listed in Table I.

As can be seen in Table I, the rate of this third process is 10–20-fold lower than that of the second. The quenching amplitude saturated at about 600 μM, but rates could be measured up to 800 μM before any appreciable aggregation took place.

We interpret the very fast phase of quenching to represent the effect of cobalt on the outer surface of the vesicles, and the first measurable exponential to represent the initial rate of entry of Co^{2+} into the interior of the SUV followed by quenching of the inner surface probes. If this second process were due to influx of Co^{2+} merely by diffusion down its concentration gradient, we would expect that the permeability constant would be independent of Co^{2+} concentration. Fig. 5 demonstrates that this is not the case.

In addition to the concentration gradient, there is a differential in surface potential produced by the initial binding of the Co^{2+} ions to the outer surface of the SUV. Conversion of the initial rate of cobalt penetration, k_1, into permeability changes were made by applying the Goldman-Hodgkin-

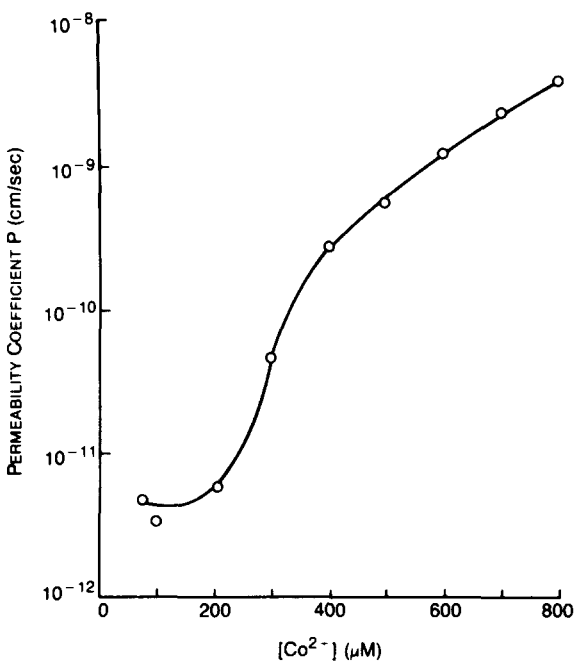

Fig. 5. Permeability rates of cobalt into PS-PE SUV were derived from Eqn. 1. The surface potentials were derived from the Stern-Gouy-Chapman theory using the appropriate binding constants as noted in the legend to Fig. 3.

Katz equation (Eqn. 6) [12,13]. At low cobalt concentrations, P is fairly constant at about 10^{-12} cm/s. This is somewhat higher than $P \simeq 10^{-14}$ cm/s for Na^+ transport through phosphatidylcholine vesicles [9] but still a reasonably small number. On the other hand, above 300 μm Co^{2+}, P rises dramatically. We presume that this is due to Co^{2+}-induced destabilization of the bilayer.

Cobalt-induced aggregation of the SUV was monitored by simultaneous measurement of the apparent absorbance changes in the samples. No detectible change could be seen below 300 μM (Fig. 4B), although this concentration was more than enough to quench all of the SUV fluorescence (Fig. 1C). Above this concentration extremely small amplitude changes were recorded. These were fitted to a single second-order process (Eqn. 3). As can be seen, the quality of the fits for the remaining data are quite poor due to the extremely low amplitudes of the changes ($\Delta A \cong 10^{-4}$ A units with bimolecular rates of under 10^{-4} s^{-1}). Complete dimerization of particles of the size of SUV should produce a $\Delta A/A_0$ of about 1 [14,15]. Thus, the Co^{2+}-induced quenching of the fluorescence seen by stopped flow is not a consequence of particle aggregation; however, the rapid change in permeability coefficient is in the same range in which we begin to see a change in A.

The rate constant for the slowest fluorescence quenching process seems to increase concomitantly with the rate constant for A changes. Although the amplitude of aggregation (and any subsequent fusion) is low, it is possible that a portion of cobalt entry is due to the leakage of PS-PE SUVs associated with fusion [8].

Mechanism of initial cobalt permeability into SUV

The results demonstrate that the large REV are normally impermeable to Co^{2+} cations. The permeability of the SUV has a number of possible explanations:

(A) The binding of Co^{2+} to the external membrane causes the fluorescent molecules on the internal leaflet to 'flip' to the external leaflet.

(B) The high radius of curvature of the SUV produces defects (pores, increased permeability) in the structure of the membrane which allows the Co^{2+} to pass through and quench the inner leaflet. These defects disappear as the radius of curvature becomes less radical; thus the larger diameter REV are not leaky.

(C) The binding of Co^{2+} to the surface induces defects on the packing of the lipids in the SUV. Defect formation allows passage of the cobalt through the membrane. These defects do not appear in LUV at the cobalt concentrations tested, presumably because of the lower radius of curvature.

Binding of Co^{2+} to the outer leaflet of the bilayer will produce a potential gradient across the membrane. Mechanism A cannot be ruled out, but seems unlikely, since we would have to assume that Co^{2+} specifically traps the fluorescently labelled lipid. However, we cannot rule out the possibility that flip-flop of lipids acts as a carrier for Co^{2+} entry.

We have noted above that, due to their very high curvature, SUV phospholipids will be distributed with 65–70% facing outward and 30–35% facing inward. In addition, the acyl chains will experience more motional freedom than in a planar or less radically curved bilayer [16]. We would expect that such a structure may contain transient or permanent defects which would allow the passage of a small molecule. The passage of the Co^{2+} through the membrane would be aided by the creation of the potential gradient when Co^{2+} binds to the outer surface. However, if the putative defects existed before the addition of the cobalt, we would expect the permeability coefficient to be independent of $[Co^{2+}]$. That this is not the case rules out mechanism II and strongly suggests that the binding of cobalt induces the formation of the defects. As noted above, analysis fo the stopped-flow data shows that the threshold of the Co^{2+} concentration required for any detectable aggregation is about 300 μM. We interpret this as the threshold for defect formation in the membrane.

These results, taken with our earlier findings [6], suggest that the SUV is not a good model for membrane fusion studies based on core-mixing assays which might yield ambiguous results due to leakage. Many biological storage granules (e.g., synaptic vesicles) have radii in the range of the SUV. These vesicles are known to be unstable upon isolation and rapidly leak their stores of neurotransmitters [17], especially if subjected to higher temperatures. Other storage organelles of

larger diameter such as chromaffin granules are quite stable at low temperatures but begin to leak when they are warmed above 6°C [18]. Although these effects may be due to the membrane proteins, it is interesting to speculate that such effects are due at least in part to the packing geometry of the lipids in the respective bilayers.

Measurement of surface potential

Membrane surface charge and resulting electrostatic potential plays an important role in a number of physiological events, including enzyme function [19], gating components of axons [20], membrane fusion [4] and membrane protein orientation [10]. Many techniques have been developed to monitor changes in surface charge induced by mono- and divalent cations, or of other agents such as anesthetics and proteins. They include direct surface potential measurements on monolayers [21], changes in capacitance and conductance of planar bilayers [22], and electrophoretic zeta-potential measurements [9]. Since the amount of Co^{2+} in the vicinity of the membrane surface is a function of surface charge, and this ion is a potent quencher of fluorescence, the technique described in this paper can be used to measure the membrane potential of a sample of known phospholipid composition in a known buffer. There are several recent reports of techniques to incorporate fluorescent phospholipids into biological membranes [23–25]. Therefore, even if the surface composition is not known, as would be the case for a biological membrane, it would still be possible to measure the relative change in surface potential due to some treatment, e.g., binding of a polyamine to a membrane surface. This is in contrast to some of the techniques mentioned above, which are limited to their applicability to model systems.

References

1 Mason, J.T. and Huang, C. (1978) Ann. NY Acad. Sci. 308, 29–49

2 Szoka, F. and Papahadjopoulos, D. (1978) Proc. Natl. Acad. Sci. USA 75, 4194–4198

3 Papahadjopoulos, D. (ed.) (1978) Ann. NY Acad. Sci. 308, 11–462

4 Blumenthal, R. (1985) Curr. Topic Membrane Transp. 27, in the press

5 Weinstein, J.N., Yoshikani, S., Henkart, P., Blumenthal, R. and Hagins, W.A. (1977) Science 195, 489–492

6 Morris, S.J., Gibson, C.C., Smith, P.D., Greif, P.C., Stirk, C.W., Bradley, D., Haynes, D.H. and Blumenthal, R. (1985) J. Biol. Chem. 260, 4122–4127

7 Knott, G.D. (1979) Computer Programs Biomed. 10, 271–280

8 Morris, S.J., Chiu, V.K.C. and Haynes, D.H. (1979) Membrane Biochem. 2, 162–202

9 McLaughlin, S., Malrine, N., Gresalfi, T., Vaio, G. and McLaughlin, A. (1981) J. Gen. Physiol. 77, 445–473

10 Weinstein, J.N., Blumenthal, R., Van Renswoude, J., Kempf, C. and Klausner, R.D. (1982) J. Membrane Biol. 66, 203–212

11 Homan, R. and Eisenberg, M. (1985) Biochim. Biophys. Acta 812, 485–492

12 Goldman, D.E. (1943) J. Gen. Physiol. 27, 37–60

13 Hodgkin, A.L. and Katz, B. (1949) J. Physiol. (London) 108, 37–77

14 Lansman, J. and Haynes, D.H. (1975) Biochim. Biophys. Acta 394, 335–347

15 Morris, S.J., Hellweg, M. and Haynes, D.H. (1979) Biochim. Biophys. Acta 553, 342–350

16 Lichtenberg, D., Freire, E., Schmidt, C.F., Barenholz, Y., Felgner, P.L. and Thompson, T.E. (1981) Biochemistry 20, 3462–3467

17 Breer, H., Morris, S.J. and Whittaker, V.P. (1978) Eur. J. Biochem. 87, 453–458

18 Sudhof, T.C. and Morris, S.J. (1983) Biochim. Biophys. Acta 730, 207–216

19 Wojtczak, L. and Nadecz, M.J. (1979) J. Biol. Chem. 94, 99–107

20 Gilbert, D.L. and Ehrenstein, G. (1969) Biophys. J. 9, 447–463

21 Bangham, A.D. and Papahadjopoulos, D. (1966) Biochim. Biophys. Acta 126, 181–184

22 Schock, P.D., Sargent, D.F. and Schwyzer, R. (1979) J. Membrane Biol. 46, 71–89

23 Owen, C.S. (1980) J. Membrane Biol. 54, 13–20

24 Tanaka, Y. and Schroit, A.J. (1983) J. Biol. Chem. 258, 11335–11343

25 Morris, S.J. and Bradley, D. (1985) Biochemistry 23, 4642–4650